Int. J. Electrochem. Sci., 16 **(2021)** Article Number: 211048, doi: 10.20964/2021.10.26

International Journal of
ELECTROCHEMICAL
SCIENCE
www.electrochemsci.org

Preparation of Activated Carbon Derived from Tobacco and its Electrochemical Properties

Zhiqian Li[1,2], *Yang Yang*[1,2], *Ruiyao Yao*[1,2], *Hongli Gao*[1,2], *Kai Song*[1,2], *Wanping Chen*[1,2], *Guoying Wang*[1,2], *Gaofeng Shi*[1,2*]

[1] School of Petrochemical Engineering, Lanzhou University of Technology, Lan gong ping Road, Lanzhou, Gansu, China
[2] Key Laboratory of Low Carbon Energy and Chemical Engineering of Gansu Province
[*]E-mail: 1138894176@qq.com

Received: 14 June 2021 / *Accepted:* 4 August 2021 / *Published:* 10 September 2021

Tobacco was carbonized two steps in KOH as an activator to produce high-performance carbon materials for supercapacitors. To make bio-carbon, tobacco was pre-carbonized at 400℃ to build a preliminary carbon skeleton, then activated with KOH and carbonized at 800℃ for 1 hour. SEM, XPS, Raman, and BET were used to check the physicochemical properties of the tobacoo porous carbon materials. In contrast, GCD, CV, and EIS were used to determine electrochemical properties. PC3's outstanding electrochemicalperformance is due to its vast surface area (1728.5 m^2/g), shortening ion diffusion routes and allowing for rapid electron migration. The tobacoo porous carbon PC3's specific capacitance is 324F/g. Thus, tobacco can be used as a material for supercapacitors and electrodes.

Keywords: Tobacco; Carbonization; electrochemical performance.

1. INTRODUCTION

Due to the constrained resource limits of traditional fossil fuels, new renewable energy sources such as hydropower, solar, wind, and nuclear energy sources are rapidly progressing and becoming increasingly popular[1,2]. However, their renewable sources could not deliver a regular power supply as the originals are variable in time [3]. Thus, the focus has been shifted to new energy sources to smooth the intermittency of the energy sources. Supercapacitor energy storage devices are not only good at storing energy, but they are also inexpensive, efficient, and convenient, as well as environmentally friendly[4,5]. In recent years, supercapacitors have been used in energy storage devices, such as distributed sensor networks and mobile electronic devices, in military and civilian applications[6–8]. Porous carbon materials have many advantages, including a large specific surface area, good cyclic stability, and a low cost. In particular, the production of electrode materials from

porous carbon biomass has become a contentious issue. The raw material exploited in this experiment was tobacco, which has a high production value in China. The two-step used in this experiment result in a produced tobacoo porous carbon with good performance. Recently, Yuxuan Liu etal[9] reported that One-step expansion procedures of tobacco stem for capacitive tobacoo stem porous carbon with a specific capacitance of 225.3F/g. The reason is that the contribution of rich self-doping of oxygen for introducing pseudo-capacitance in tobacoo stem porous carbon. In this paper, tobacco was first used to make electrode materials via the two-step method. The reason why tobacoo porous carbon PC3 hassuperior capacitive performance is that the successful two-steps carbonized.

2. EXPERIMENTAL

2.1. Equipment and Reagents

KOH (AR), HCl (36%), acetylene black(AR), polytetrafluoroethylene(2%), ethanol absolute (AR), Ultrapure water;Crusher, tube furnace, vacuum drying oven(KZ-82), CHI660E workstation, electronic balance(BS-201S)

2.2. Experimental process

Tobacco was ground into a fine powder. 5g of tobacoo was heated at 400℃ for 60 minutes in the absence of oxygen in a tube furnace. Following that, different mass ratios of KOH (1:0; 2:1; 1:1; 1:1.5) were used for blending and grinding. PC1, PC2, PC3, PC4 were assigned to the prepared samples.

PC1, PC2, PC3, PC4 were carbonized for 60 minutes at 800 ℃ with a 600℃/h increasing rate in the absence of oxygen in a tube furnace. The tobacoo porous carbon was immersed in hydrochloric acid solution (12%) for 12 hours and neutralized with ultrapure water, last baked in an oven at 70 ℃ for 12 hours.

2.3. Material Characterization

The BET analysis of the tobacoo porous carbon were measured by a surface analyzer at 77 K.The XRD analysis examine the crystal structure of the tobacoo porous carbon. The tobacoo porous carbon’s Raman spectrum was measured using a spectrometer. The XPS analysis was investigated to determine the elements’ composition in the tobacoo porous carbon. The SEM were used to examine the surface structure of the tobacoo porous carbon.

2.4. Electrochemical measures

The electrode was prepared by mixing the acetylene black, polytetrafluoroethylene, tobacoo porous carbon with a weight ratio of 1:3:20. Then it was thoroughly combined and coated with foam

Ni grids to cover the 10×10 mm zone, then baked for 14 hours in a drying oven[9]. The tablet device was then pressed for 50 seconds at an 8 MPa pressure. The specific capacitance C was calculated from the GCD [10,11]:

$$Cs = \frac{I\Delta t}{m\Delta V}$$

I is the tobacoo porous carbon's discharge current (A), *m* is the mass of the tobacoo porous carbon (g), *Δt* is the discharge time (s) of the tobacoo porous carbon, *ΔV* is the the tobacoo porous carbon's potential window (V) .

3. RESULTS AND DISCUSSION

3.1. BET analysis of tobacoo porous carbon

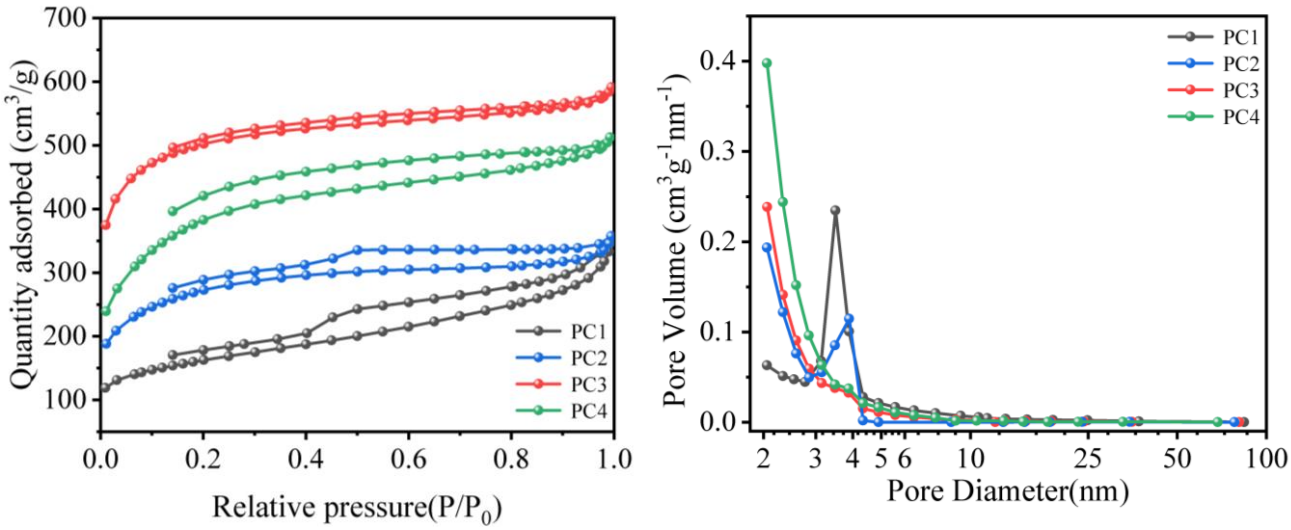

Figure 1. BET isotherms (A), and the tobacoo porous carbon's pore size distribution (B)

Table 1. S_{BET} , V_T ,V_M data of the tobacoo porous carbon

Name ID	S_{BET} (m^2g^{-1})	V_T (cm^3g^{-1})	V_M (cm^3g^{-1})
PC1	565.67	0.47	0.10
PC2	957.25	0.51	0.17
PC3	1728.50	0.88	0.49
PC4	1373.70	0.76	0.14

PC3, mass ratios of KOH 1:1; S_{BET}, specific surface area.

The porous properties of tobacoo porous carbon in processed biomass have been investigated. PC1, PC2, PC3, and PC4 had surface areas of 565.67 m^2/g, 957.25 m^2/g, 1728.50 m^2/g, and 1373.70 m^2/g, respectively to the data.Figure.1A shows the BET curve of porous carbon, the adsorption volume

of sample PC3 decreased considerably at lower relative pressure, indicating the presence of micropores in tobacoo porous carbon; a retention ring emerged for nitrogen adsorption, indicating the presence of mesopores at higher relative pressure[12–14]. As can be seen in Figure.4B, the PC3 has an average pore diameter of 2.05 nm, indicating that it is a micropores material[15]. The PC3 has the most defined pore structure. PC3 has a total pore volume of 0.88 L/kg and a microspore volume accounting for 55.60 percent of the total tobacoo porous carbon pore volume. This suggests that the structure of tobacoo porous carbons are mainly microporous.

3.2. XRD and Raman spectra of tobacoo porous carbon

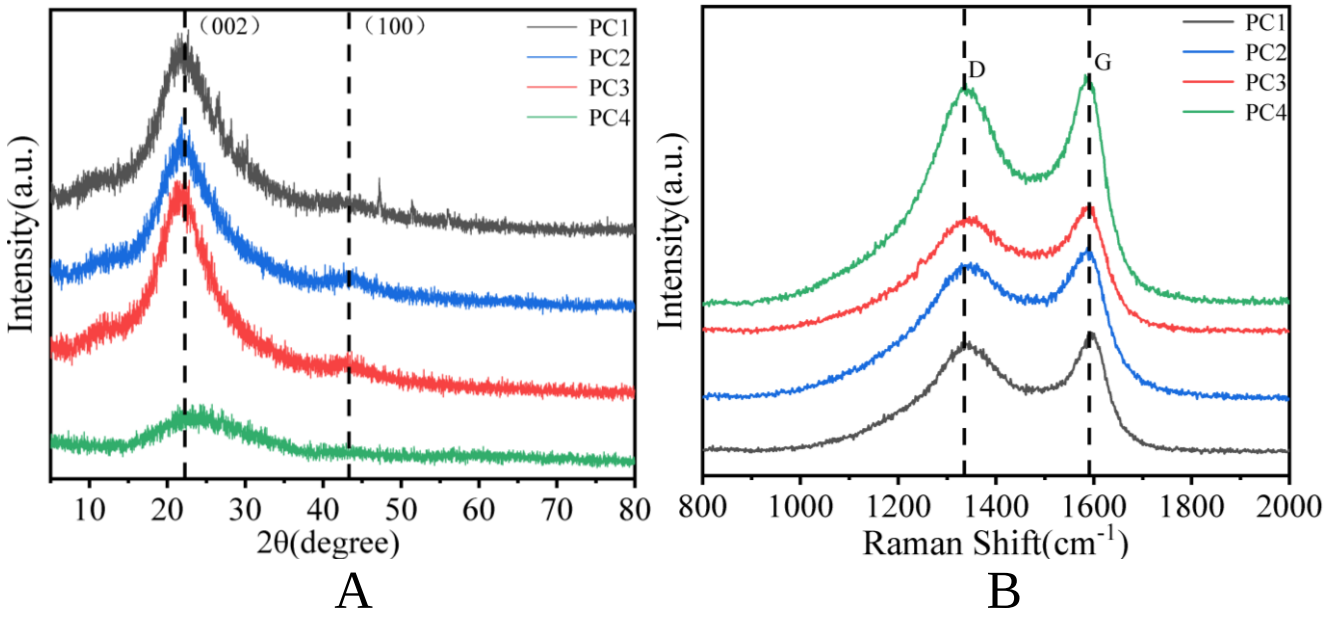

Figure 2. Tobacoo porous carbon's Raman image (A), Tobacoo porous carbon's XRD image (B)

As shown in Figure.3A, the tobacoo porous carbon's graphite-layer crystal plane exhibit one apparent distinctive peaks at 22.5°and the tobacoo porous carbon's amorphous-carbon crystal plane exhibit another apparent distinctive peaks at 43.5° in the produced carbon materials[16]. Furthermore, no other miscellaneous peaks occurred, indicating that the manufactured carbon contained little impurities and was of high purity.

In Figure.3B, peak D represents atomic lattice defects and the D peak of the tobacoo porous carbon at 1340cm^{-1}, and peak G represents the C atom in sp^2 hybridization's in-plane stretching vibration and the G peak of the tobacoo porous carbon at 1590cm^{-1}[16]. In porous carbon materials, I_D / I_G [17,18] measures the graphitization and the degree of structural disorder. PC1, PC2, PC3, and PC4 had I_D / I_G values of 0.94, 0.95, 0.97,and 0.96, respectively, indicating that the tobacoo porous carbon following activation without KOH has a low degree of disorder.

3.3. SEM of tobacoo porous carbon

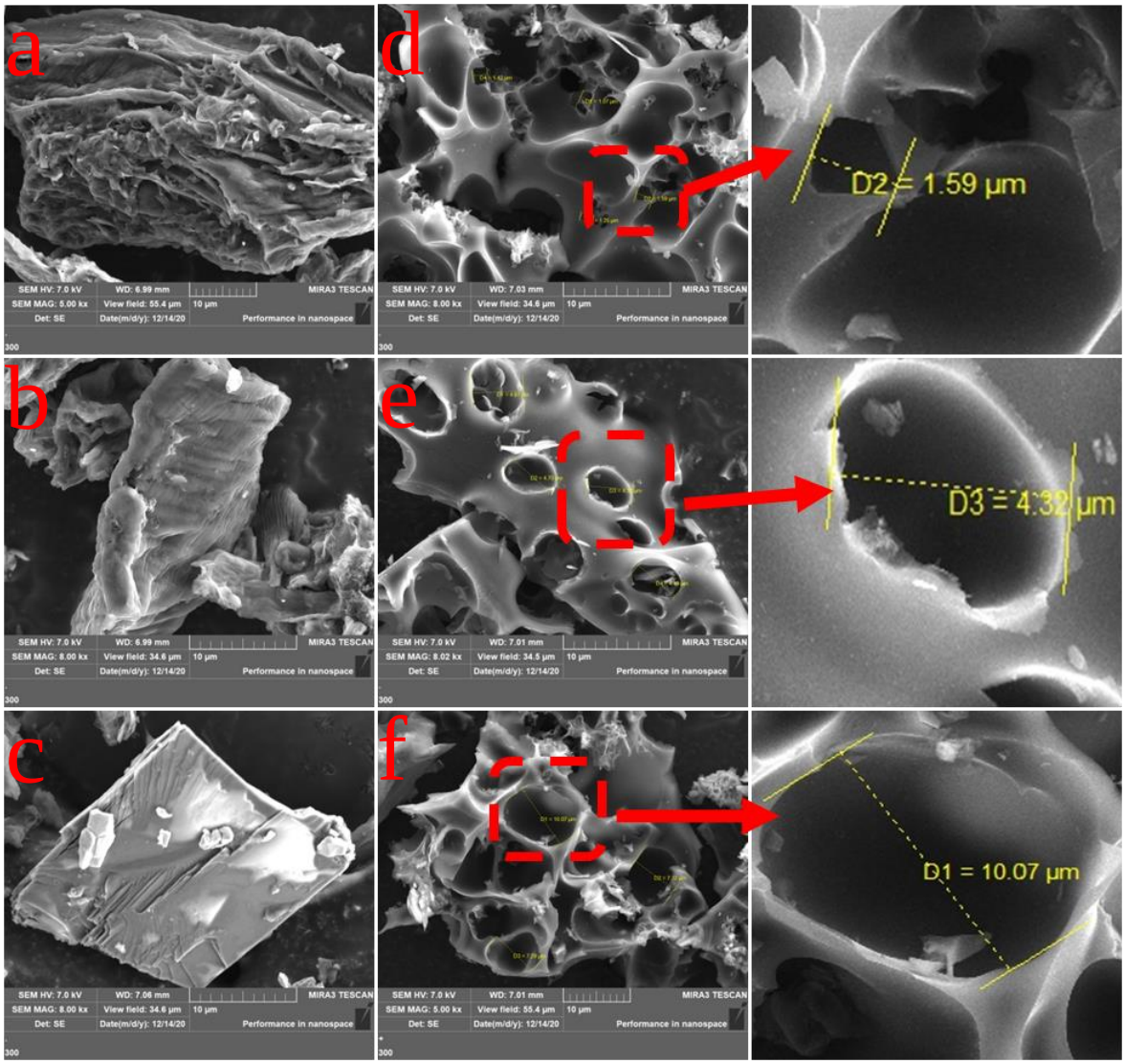

Figure 3. PC1's SEM (a-c), PC3's SEM (d-f)

Figure 3(a-c) shows that tobacco materials have essentially no pores, whereas Figure 3(d-f) shows that the porous carbon has huge pores. It's a porous graded carbon with better electrochemical properties. This material has a variety of macropores at 10, 5 and 1 micron respectively, which is beneficial for electrochemical applications. The reason why a more porous structure is that the tobacoo porous carbon layer structure being destroyed during the activation.

3.4. XPS spectrum of tobacoo porous carbon

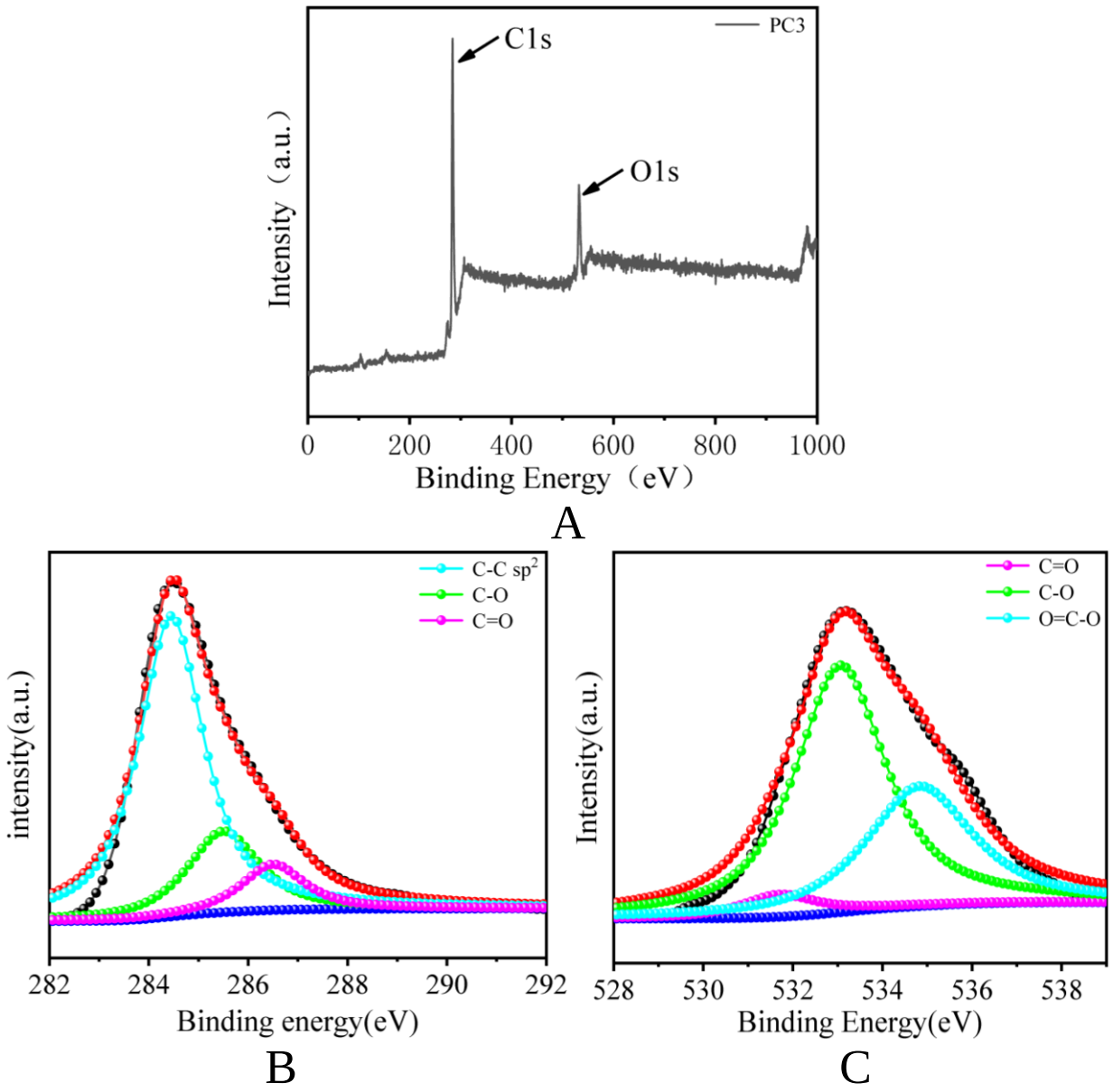

Figure 4. tobacoo porous carbon PC3's XPS spectra (A), and the C1s and O1s's XPS spectra (B-C).

Figure.4A is the full spectrum of tobacoo porous carbon PC3. Results show that the tobacoo porous carbon PC3 was composed of 84.55% of C element and 15.55% of O element. In figure.4B, there are mainly C=O bond (286.5 eV) and a small amount of C-O bond (285.5 eV) and C=C bond (284.6 eV)[19,20] in the tobacoo porous carbon PC3. In figure.4C, there are mainly C-O bond (532.7 eV)[21] and a small amount of O=C-O bond (533.7 eV) and C=O bond (531.6 eV)[21] in the tobacoo porous carbon PC3. In heat treatment, the peak of the C–O bond formed at 532.7 eV [22]. It is well known that as the number of functional groups increases, the possibilities for loading and modification of the tobacoo porous carbon increase in the future.

3.5. Electrochemical performance of tobacoo porous carbon

With a three-electrode device and a 6 M KOH, the sample output was estimated. In figure.5A, it shows the GCD of three tobacoo porous carbon of 0.5 A/g, with capacitances of 199.55, 324.2, and 137.15 F/g for the tobacoo porous carbon PC2, PC3, and PC4, respectively. PC3 is the best tobacoo porous carbon; In figure.5B, it shows the CV curves of tobacoo porous carbon of 10mV/s; They all look like a rectangle, implying that they share electrical double-layer capacitance properties. The tobacoo porous carbon PC3 has the most significant area. Figure.5E demonstrates the EIS curves of three tobacoo porpos carbon [23–25]. In the high-frequency area, the tobacoo porous carbon PC2, PC4 radius are small. It shows that the electrochemical resistance of the tobacoo porous carbon PC2, PC4 are very strong. At the same time, in the high-frequency region, the tobacoo porous carbon PC3 has a large radius. The low-frequency region of tobacoo porous carbon PC3 is almost vertical. It shows that the electrochemical resistance of the tobacoo porous carbon PC3 is very weak. That means the tobacoo porous PC3's specific capacitance is greater than the tobacoo porous PC2, PC4.

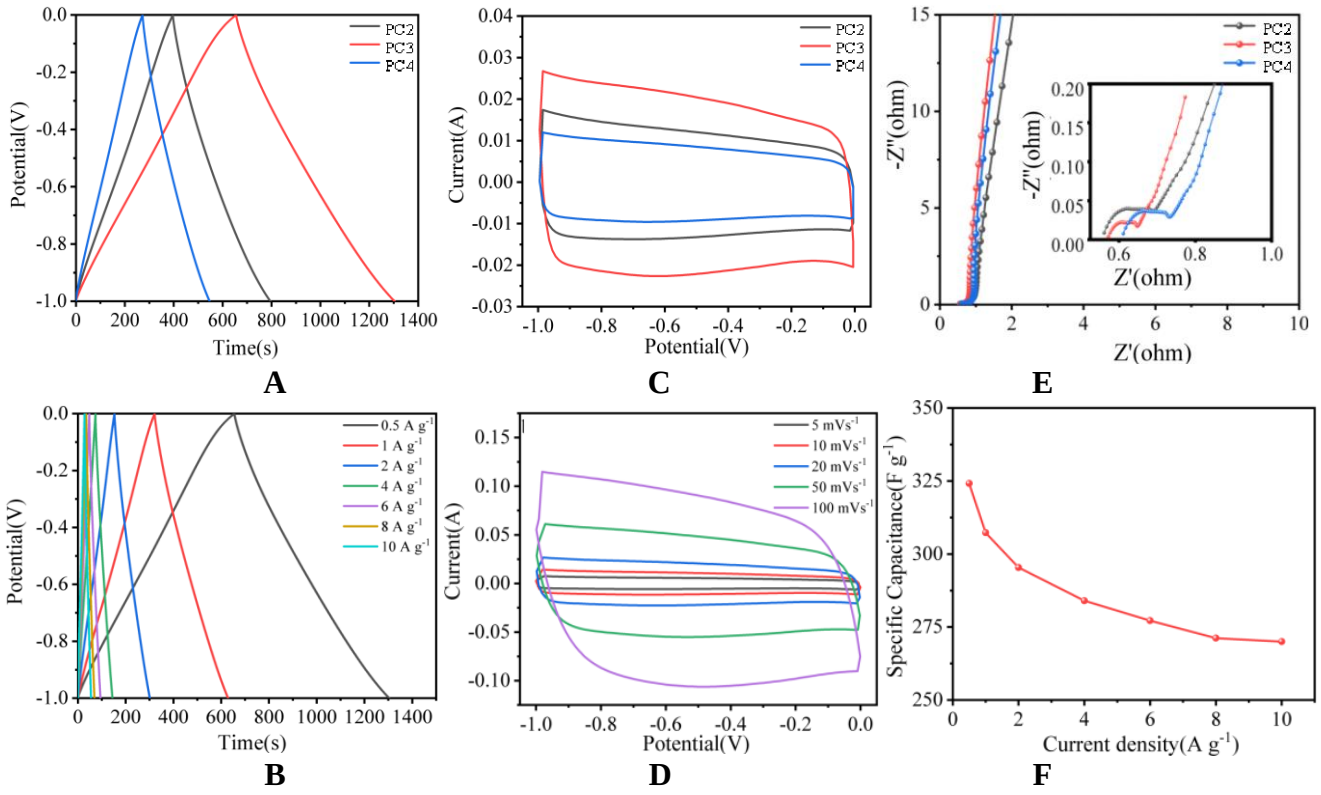

Figure 5. GCD curves of the tobacoo porous carbon of 0.5A/g (A), and different current densities (B), CV curve of the tobacoo porous carbon of 10mV/s (C), and 5-100 mV/s (D), nyquist plots of the tobacoo porous carbon (E), the influence of current densitiy on the tobacoo porous carbon specific capacitance (F)

This shows that, in comparison to PC3, the other two tobacoo porous carbons have high internal resistance. In terms of capacitance reliability, the PC3 have low charge transfer resistance and offers the best performance. In Figure.5D, it can maintain a rectangular-like shape of the tobacoo

porous carbon PC3 at varied scanning rates of 5 mV/s to 0.1 V/s, as illustrated. In Figure.5F, The specific capacitance retention rate is 83%.

Table 2. Comparison of this work with other work

Material	Environment	C(F/g)	Reference
yellow horn	6 M KOH	246.5 (1 Ag^{-1})	[14]
Camellia	2M KOH	205 (0.5 Ag^{-1})	[19]
rice straw	1M Na_2SO_4	400(0.1 Ag^{-1})	[23]
Licorice	6 M KOH	320(0.5 Ag^{-1})	[24]
Peanut shells	1 M H_2SO_4	340 (0.25 Ag^{-1})	[26]
Fujimoto bean	6M KOH	219(1 Ag^{-1})	[27]
Corncob	6M KOH	120(1 Ag^{-1})	[28]
Rice husks	6 M KOH	233 (2 Ag^{-1})	[29]
bean curd stick	6 M KOH	405 (0.5 Ag^{-1})	[30]
corn stalk core	6 M KOH	323 (0.1 Ag^{-1})	[31]
Tobacco	6M KOH	324(0.5 Ag^{-1})	**This work**

4. CONCLUSION

In this experiment, tobacco was employed as a carbon source, and was carbonized two steps in KOH as an activator to produce high-performance carbon materials for supercapacitors. The surface area of the tobacoo porous carbon PC3 was 1728.5 m^2/g, with the tobacoo porous carbon total pore volume of 0.88 L/kg, indicating that KOH had a high pore expansion efficiency. The tobacoo porous caobon's specific capacitance is 324 F/g of 0.5 A/g. The tobacoo porous caobon's retention rate rises to 83% as the recent density increases from 500 mA/g to 10000 mA/g. As a result, the findings imply that tobacoo is an excellent suitable carrier for tobacco-based energy production.

NOTES
No potential conflict of interest relevant to this article was reported

References

1. S. Lei, L. Chen, W. Zhou, P. Deng, Y. Liu, L. Fei, W. Lu, *J. Power Sources*, 379 (2018) 74–83.
2. Y. Hu, X. Li, G. Wang, F. Luo, K. Yi, Y. Iradukunda, G. Shi, *Int. J. Electrochem. Sci.*, 16 (2021) 1–12.
3. J. Rantanen, *J. Pharm. Pharmacol.*, 59 (2007) 171–177.
4. C. Ma, R. Wang, Z. Xie, H. Zhang, Z. Li, J. Shi, *J. Porous Mater.*, 24 (2017) 1437–1445.
5. W. Li, F. Zhang, Y. Dou, Z. Wu, H. Liu, X. Qian, D. Gu, Y. Xia, B. Tu, D. Zhao, *Adv. Energy Mater.*, 7 (2011) 382–386.
6. X.Q. Wenting Li, Zelin Li, Chao Zhang, Wei Liu, Ce Han, Baijun Yan, Shengli An, *Solid State*

Ion., 351 (2020) 115319.
7. X.Z. Feng Chen, Jiangang Ren, Lulu Ma, Xinyu Luo, Nana Wu, Shenke Ma, Bing Li, Zhiming Song, 1, *Int. J. Electrochem. Sci.*, 15 (2020) 5803–5820.
8. G. Wang, Y. Iradukunda, G. Shi, P. Sanga, X. Niu, Z. Wu, *J. Environ. Sci. (China)*, 99 (2021) 324–335.
9. L. Yuxuan, C. Xinhua, Z. Shenghui, *J. Porous Mater.*, 1 (2021) 1–14.
10. X. Zhao, P. Li, S. Yang, Q. Zhang, H. Luo, *Ionics (Kiel).*, 23 (2017) 1–10.
11. M. Yu, T. Zhai, X. Lu, X. Chen, S. Xie, W. Li, C. Liang, W. Zhao, L. Zhang, Y. Tong, *J. Power Sources*, 239 (2013) 64–71.
12. Y. Ou, C. Peng, J. Lang, D. Zhu, X. Yan, *Carbon N. Y.*, 29 (2014) 193–202.
13. H. Lu, W. Dai, M. Zheng, N. Li, G. Ji, J. Cao, *J. Power Sources*, 209 (2012) 243–250.
14. F. Luo, Y. Iradukunda, K. Yi, Y. Hu, X. Li, G. Wang, G. Shi, *Int. J. Electrochem. Sci.*, 16 (2021) 1–12.
15. G. Shi, C. Liu, G. Wang, X. Chen, L. Li, X. Jiang, P. Zhang, Y. Dong, S. Jia, H. Tian, Y. Liu, Z. Wang, Q. Zhang, H. Zhang, *Ionics (Kiel).*, 25 (2019) 1805–1812.
16. H. Hongying, L. Chengyi , Yu Xianxi, Y. Yuan, D. Zhipeng, L. Dongdong, *Ournal Mater. Cycles Waste Manag.*, 21 (2019) 1123–1131.
17. Y. Iradukunda, G. Wang, X. Li, G. Shi, Y. Hu, F. Luo, *J. Energy Storage*, 39 (2021) 102577.
18. D. Zhang, M. Han, Y. Li, J. He, B. Wang, K. Wang, H. Feng, *J. Power Sources*, 372 (2017) 260–269.
19. C. Lu, J. Li, J.P. Cheng, *J. Power Sources*, 394 (2018) 9–16.
20. H. Chen, Yan-chuan Guo, F. Wang3, G. Wang4, P.Q. 1, 4, Xuhong Guo 1, *New Carbon Mater.*, 32 (2017) 592–599.
21. N. Jung, K. Soongeun, D. Lee, D.-M. Yoon, Y.M. Park, A. Benayad, J.-Y. Choi, jong S. Park, *Adv. Mater.*, 5 (2013) 1–12.
22. O. Sedahmed, A. Raja, Senthil, J. Pan, Y. Sun, *J. Power Sources*, 414 (2019) 401–411.
23. H. Jin, J. Hu, S. Wu, X. Wang, H. Zhang, H. Xu, *J. Power Sources*, 384 (2018) 270–277.
24. K. Yi, Y. Iradukunda, F. Luo, Y. Hu, X. Li, G. Wang, G. Shi, *Int. J. Electrochem. Sci.*, 16 (2021) 1–10.
25. Y. Iradukunda, G. Wang, X. Li, G. Shi, A. Ismail, M. Albashir, L. Dusengemungu, Y. Hu, F. Luo, K. Yi, X. Niu, Z. Wu, *J. Electroanal. Chem.*, 890 (2021) 115228.
26. Heard.E, Dwayne, PillingJ., Michael, *Chem. Rev.*, 103 (2003) 5163–5198.
27. G. Shi, Z. Wang, C. Liu, G. Wang, S. Jia, X. Jiang, Y. Dong, Q. Zhang, *Int. J. Electrochem. Sci.*, 14 (2019) 5259–5270.
28. W.-H. Qu, Y.-Y. Xu, A.-H. Lu, X.-Q. Zhang, W.-C. Li, *Bioresour. Technol.*, 189 (2015) 285–291.
29. X. He, P. Ling, M. Yu, X. Wang, X. Zhang, M. Zheng, *Electrochim. Acta*, 105 (2013) 635–641.
30. L. Shi, L. Jin, Z. Meng, Y. Sun, C. Li, Y. Shen, *RSC Adv.*, 8 (2018) 39937–39947.
31. Y. Cao, K. Wang, X. Wang, Z. Gu, Q. Fan, W. Gibbons, J.D. Hoefelmeyer, P.R. Kharel, M. Shrestha, *Electrochim. Acta*, 212 (2016) 839–847.